Original Research Paper

Assessment and prediction of tablet properties using transmission and backscattering Raman spectroscopy and transmission NIR spectroscopy

CrossMark

Elisabeth Peeters [a,1], *Ana Filipa Tavares da Silva* [b,c,1], *Maunu Toiviainen* [d],
Jeroen Van Renterghem [b], *Jurgen Vercruysse* [a], *Mikko Juuti* [d], *Joao Almeida Lopes* [c],
Thomas De Beer [b], *Chris Vervaet* [a,*], *Jean-Paul Remon* [a]

[a] *Laboratory of Pharmaceutical Technology, Ghent University, Ottergemsesteenweg 460, 9000 Ghent, Belgium*
[b] *Laboratory of Pharmaceutical Process Analytical Technology, Ghent University, Ottergemsesteenweg 460, 9000 Ghent, Belgium*
[c] *REQUIMTE, Department of Chemical Sciences, University of Porto, Rua de Jorge Viterbo Ferreira, 228, 4050-313 Porto, Portugal*
[d] *VTT Technical Research Centre of Finland, Optical Measurement Technologies, Kaitoväylä 1, 90570 Oulu, Finland*

ARTICLE INFO

ABSTRACT

This study investigated whether Raman and Near Infrared (NIR) spectroscopy could predict tablet properties. Granules were produced on a continuous line by varying granulation parameters. Tableting process parameters were adjusted to obtain uniform tablet weight and thickness. Spectra were collected offline and tablet properties determined with traditional analyzing methods. Partial Least Squares (PLS) regression was used to correlate spectral information to tablet properties, but predictive models couldn't be established. Principal component analysis (PCA) was effectively used to distinguish theophylline concentrations and hydration levels and multiple linear regression (MLR) analysis allowed insight on how granulation parameters affect granule and tablet properties.

© 2016 Shenyang Pharmaceutical University. Production and hosting by Elsevier B.V. This is an open access article under the CC BY-NC-ND license (http://creativecommons.org/licenses/by-nc-nd/4.0/).

1. Introduction

Most pharmaceutical manufacturing nowadays is still performed using batch manufacturing processes. In contrast to other industries (e.g. petrochemical, chemical and food industries) that transferred to continuous manufacturing decades ago, the pharmaceutical industry has been reluctant to move from batch processing toward continuous processing. Rigorous regulatory constraints, among others, can be identified as one of the reasons for this [1–6]. However, since the publication of the United States Food and Drug Administration's (FDA) Pharmaceutical current Good Manufacturing Principles (cGMPs) for the 21st century initiative, there has been a shift toward regulatory authorities encouraging the pharmaceutical industry to implement new technology. The International Conference on Harmonization (ICH) guidelines Q8 [7], Q9 [8] and Q10 [9] together with the Process Analytical Technology (PAT) – Guidance for Industry [10] and the Process Validation – Guidance for Industry [11] introduced the concepts of Quality by Design (QbD) and the use of science and risk-based approaches to assure product quality [1].

The production of tablets on a high speed rotary tablet press is by definition a classic example of a continuous process. As long as the machine is fed with material, tablets will be produced and ejected at the ejection station. The production speed of an industrial tablet press gives an extremely large output (i.e. several hundreds of thousands of tablets per hour). If analyzing methods guaranteeing the quality of the end product are optimized, this results in a shorter "time-to-market" and a cost and floor space reduction, as there is less need for storage. In theory, however, tablet quality is still mainly assessed offline by performing traditional methods of analysis on tablets collected at the end of production. These methods are often destructive and involve sample pretreatment. As a consequence, the latter becomes the rate-limiting step and annuls the advantages of the fast continuous production process. Consequently, to allow real-time release, other techniques are necessary. Evidently, the use of PAT-tools is a vital element in this process.

In contrast to the classical analyzing methods, spectroscopic techniques offer a rapid, simple, non-invasive and non-destructive alternative requiring little or even no sample preparation. Near Infrared (NIR) and Raman spectra carry significant chemical and physical features of the samples but since these often overlap it is difficult to get information directly from the spectra. Therefore, multivariate data analysis tools such as Principal Component Analysis (PCA) are essential to extract and summarize this information [12]. NIR reflectance and also transmittance measurements have been reported as reliable methods for the identification and quantification of active pharmaceutical ingredients (APIs) in tablets [13]. NIR spectroscopy has also already been used for the prediction of tablet hardness [14–18], porosity [19] and disintegration time [20] of tablets prepared at different compression forces. Some publications also reported about the application of Raman spectroscopy to determine tablet properties [12,19,21]. Wang et al. [21] and Johansson et al. [12] studied the use of Raman spectroscopy in the prediction of tablet hardness. Raman spectroscopy was also used by Shah et al. [19] to predict the porosity of ex-

tended release matrix tablets. It is crucial to emphasize that all of these studies were performed on tablets prepared using different compression forces, hence resulting in tablets with a different thickness or a different weight, depending on the followed approach (i.e. maintaining the weight yields tablets with lower thickness at higher compression force, whereas maintaining the thickness requires a higher weight when the compression force is increased). Moreover, the ranges used in these studies are rather broad; e.g., Johansson et al. [12] varied the compression force from 5 to 20 kN with increments of 5 kN. Other authors used ranges with the highest force being three-fold [14], sixfold [15–20] or tenfold [13] higher compared to the lowest applied compression force. Such a wide span in compression force induces significant differences in the extent of bonding, which forms the basis of spectroscopic models to predict tablet hardness, porosity and disintegration time. However, in an industrial manufacturing process (which was mimicked in our study) the main objective is to maintain the preset tablet weight, thickness and diameter. Since the quality constraints are stringent and the rejection limits are often narrow, the properties of tablets, which do not conform to the preset specifications (i.e. within-spec tablets), will generally not differ to the extent reported in other papers. Furthermore, as differences in weight, thickness and diameter are also known to affect signals detected *via* Raman and NIR spectroscopy, it was the objective of this study to adjust the tableting process parameters to obtain for all batches tablets of uniform weight, thickness and diameter. Hence, any differences observed in tablet characteristics could only be due to the differences in granule characteristics.

The primary objective of the present study was to determine the applicability of NIR and Raman spectroscopy in the prediction of the physical properties of tablets, using the Partial Least Squares (PLS) approach. It was further investigated if these PAT-tools could also be used with the same capability to determine the concentration and hydrate level of the API (theophylline). Moreover, the influence of different granulation parameters on granule quality attributes, tablet quality attributes and associated tableting process parameters was studied.

2. Materials and methods

2.1. Materials

Theophylline anhydrate was selected as model API and purchased from Farma-Química Sur (Malaga, Spain). α-lactose monohydrate 200 M (Caldic, Hemiksem, Belgium) was used as filler for granulation and polyvinylpyrrolidone (PVP) (Kollidon®30, BASF, Ludwigshafen, Germany) in a concentration of 2.5% (w/w to the dry powder) as binder. Distilled water was used as the granulation liquid.

2.2. Preparation of powder mixtures

Before granulation, three premixes, with different theophylline concentrations (Table 1), were prepared by low shear mixing (20 min, 25 rpm) in a 20 l stainless steel drum with a filling

Table 1 – Overview of factor settings and characterization of granules and tablets from the experimental design.

Run	Batch code	Factors				Responses of granules						Responses of tablets					Tableting parameters		
		Formulation	SC	BT	LFR	Fines	Oversizedd	Friab	ρ_{bulk}	ρ_{tapped}	CI	TS	Friab	Disint	ε	VC W	FD	MCF	VC MCF
5	1111	19.50 / 78.00 / 2.50	1×4	25	36.2	34.1	9.0	19.7	0.403	0.464	13.1	1.5	0.2	199	26.1	1.9	10.00	6.63	14.5
33	1112	19.50 / 78.00 / 2.50	1×4	25	41.2	21.2	17.4	15.4	0.437	0.492	11.2	0.9	4.7*	112	25.4	1.7	9.80	5.61	19.4
3	1113	19.50 / 78.00 / 2.50	1×4	25	46.3	10.5	29.0	10.5	0.415	0.464	10.6	0.9	3.7*	188	29.0	1.6	9.35	5.41	13.5
26	1121	19.50 / 78.00 / 2.50	1×4	35	36.2	32.1	9.4	16.7	0.432	0.491	12.1	1.2	3.0*	144	28.2	1.6	9.05	5.50	19.5
25	1122	19.50 / 78.00 / 2.50	1×4	35	41.2	20.1	16.5	15.6	0.433	0.497	12.9	0.8	8.6*	108	30.4	1.7	9.05	5.68	17.4
4	1123	19.50 / 78.00 / 2.50	1×4	35	46.3	14.9	23.3	11.1	0.399	0.456	12.6	0.8	10.9*	195	31.0	2.2	9.30	5.06	12.4
34	1211	19.50 / 78.00 / 2.50	2×6	25	36.2	23.4	11.8	14.5	0.448	0.501	10.5	1.2	3.1*	220	22.3	1.9	9.20	5.76	17.1
20	1212	19.50 / 78.00 / 2.50	2×6	25	41.2	16.1	19.4	10.9	0.438	0.494	11.4	1.3	0.2	272	28.8	1.8	9.28	5.27	18.9
7	1213	19.50 / 78.00 / 2.50	2×6	25	46.3	8.9	37.4	6.5	0.446	0.519	14.1	0.8	8.3*	178	30.0	1.7	9.05	6.11	12.2
8	1221	19.50 / 78.00 / 2.50	2×6	35	36.2	20.0	16.2	12.3	0.452	0.509	11.2	0.9	2.9*	218	29.4	1.8	8.90	6.00	22.4
6	1222	19.50 / 78.00 / 2.50	2×6	35	41.2	9.6	32.4	10.3	0.442	0.495	10.6	0.7	4.9*	175	31.5	1.7	9.00	5.06	18.2
1	1223	19.50 / 78.00 / 2.50	2×6	35	46.3	4.9	43.0	4.3	0.464	0.516	10.0	1.1	0.5	526	21.4	1.5	8.50	6.03	22.3
29	2111	29.25 / 68.25 / 2.50	1×4	25	36.2	36.5	7.8	19.7	0.451	0.496	9.0	1.9	0.1	436	24.8	2.0	9.10	5.22	22.2
19	2112	29.25 / 68.25 / 2.50	1×4	25	41.2	29.7	11.5	24.7	0.409	0.441	7.3	2.1	0.1	379	27.2	2.0	9.50	5.63	27.9
17	2113	29.25 / 68.25 / 2.50	1×4	25	46.3	16.6	23.9	15.3	0.439	0.489	10.2	1.9	0.4	355	27.0	2.1	9.50	5.70	23.0
35	2121	29.25 / 68.25 / 2.50	1×4	35	36.2	35.8	7.8	18.8	0.455	0.517	11.9	2.0	0.2	346	20.7	2.1	9.10	5.60	19.2
22	2122	29.25 / 68.25 / 2.50	1×4	35	41.2	23.9	15.5	17.3	0.450	0.513	12.2	2.1	0.1	423	27.2	1.9	8.90	5.47	22.3
14	2122R1○	29.25 / 68.25 / 2.50	1×4	35	41.2	22.9	15.9	17.5	0.450	0.504	10.7	2.1	0.1	570	26.5	1.8	9.90	5.95	21.0
30	2123	29.25 / 68.25 / 2.50	1×4	35	46.3	20.1	14.9	10.8	0.401	0.456	12.0	1.8	1.1*	413	22.7	1.9	9.35	5.63	20.3
12	2211	29.25 / 68.25 / 2.50	2×6	25	36.2	33.4	7.6	14.8	0.463	0.517	10.5	2.1	0.3	519	26.8	1.9	8.72	5.56	22.5
28	2212	29.25 / 68.25 / 2.50	2×6	25	41.2	26.0	9.0	12.2	0.467	0.517	9.7	1.7	1.4*	559	22.6	2.0	8.75	5.23	23.0
23	2213	29.25 / 68.25 / 2.50	2×6	25	46.3	18.2	15.0	9.3	0.487	0.549	11.3	1.4	2.2*	382	27.6	1.7	8.63	5.57	19.1
2	2221	29.25 / 68.25 / 2.50	2×6	35	36.2	26.2	10.2	18.5	0.438	0.483	9.2	2.2	0.4	379	23.3	2.0	9.10	5.73	22.4
13	2222	29.25 / 68.25 / 2.50	2×6	35	41.2	18.2	17.9	9.2	0.469	0.529	11.3	1.9	0.5	589	25.9	1.9	9.00	5.65	20.4
10	2223	29.25 / 68.25 / 2.50	2×6	35	46.3	14.3	17.9	7.5	0.464	0.533	12.9	1.4	2.4*	388	30.1	2.2	9.60	4.98	20.2
18	3111	39.00 / 58.50 / 2.50	1×4	25	36.2	40.0	6.2	25.9	0.369	0.432	14.6	1.7	0.3	963	27.6	1.9	10.05	5.76	13.5
37	3112	39.00 / 58.50 / 2.50	1×4	25	41.2	27.3	12.9	25.1	0.417	0.479	12.9	1.6	0.1	927	21.3	2.2	9.85	5.45	18.8
36	3113	39.00 / 58.50 / 2.50	1×4	25	46.3	26.2	11.0	18.1	0.406	0.457	11.2	2.0	0.1	960	21.3	2.0	9.75	5.42	23.6
16	3121	39.00 / 58.50 / 2.50	1×4	35	36.2	36.7	7.5	22.8	0.407	0.466	12.7	2.2	0.1	653	28.0	1.9	9.75	5.57	17.2
27	3122	39.00 / 58.50 / 2.50	1×4	35	41.2	26.1	11.8	23.4	0.412	0.463	11.0	2.4	0.1	594	26.0	2.1	9.42	5.55	29.0
9	3123	39.00 / 58.50 / 2.50	1×4	35	46.3	22.8	14.3	16.9	0.417	0.456	8.6	2.0	0.2	768	28.5	2.3	9.45	5.75	19.9
31	3211	39.00 / 58.50 / 2.50	2×6	25	36.2	43.3	4.4	16.2	0.470	0.523	10.2	2.3	0.1	972	23.8	2.4	8.75	5.79	16.8
24	3212	39.00 / 58.50 / 2.50	2×6	25	41.2	28.2	8.1	16.3	0.473	0.528	10.4	2.4	0.1	571	27.1	1.9	8.70	5.60	20.5
32	3213	39.00 / 58.50 / 2.50	2×6	25	46.3	18.2	13.4	9.1	0.474	0.539	12.1	2.3	0.1	1129	22.9	2.1	9.00	5.42	23.3
21	3221	39.00 / 58.50 / 2.50	2×6	35	36.2	29.1	7.6	16.0	0.440	0.496	11.4	2.6	0.2	935	27.6	2.2	9.30	5.23	23.9
11	3222	39.00 / 58.50 / 2.50	2×6	35	41.2	21.3	13.9	14.8	0.435	0.487	10.7	1.8	0.2	1340	27.2	2.0	9.46	5.60	24.8
15	3223	39.00 / 58.50 / 2.50	2×6	35	46.3	15.8	14.2	12.1	0.451	0.489	7.8	1.6	0.1	1576	27.6	1.7	9.40	6.38	15.8

Formulation: API/lactose/PVP (%)(w/w); SC, number of kneading elements; BT, barrel temperature (°C); LFR, liquid feed rate (g/min); Fines, <300 μm (%); Oversized, >2000 μm (%); Fria, friability (%); ρ_{bulk}, bulk density (g/ml); ρ_{tapped}, tapped density (g/ml); CI, compressibility index (%); TS, tensile strength (MPa); Disint, disintegration time (s); ε, porosity (%); VC W, variation coefficient weight (%); FD, fill depth (mm); MCF, main compression force (kN); VC MCF, variation coefficient MCF (%).

○ at "Batch code" refers to the repetition of the center point.

* at "Fria" depicts the tablet batches that failed the friability test. The values of the responses/parameters are the average of all tablets in each batch.

degree of 60%, using a tumbling mixer (Inversina, Bioengineering, Wald, Switzerland).

2.3.   Granulation

Granulation experiments were performed using a high-shear co-rotating twin screw granulator, being the granulation unit of the ConsiGma™-25 continuous powder-to-tablet line (GEA Pharma Systems - Collette™, Wommelgem, Belgium), which has already been thoroughly described by other authors [1,4,6,22,23]. Depending on the experiment (Table 1), the concentration of theophylline (API conc), liquid feed rate (LFR), barrel temperature (BT) and amount of kneading elements (screw configuration (SC)) were changed [4]. The powder premix was gravimetrically dosed at a constant feed rate of 25 kg/h onto the screws (950 rpm) and the granulation liquid (distilled water) was pumped into the screw chamber in front of the first kneading element by two peristaltic pumps. After a calibration time of 60 sec, for each run 600 g of granules was collected at the outlet of the granulator. The wet granules were spread on a tray and oven-dried at 40 °C during 24 h. After drying, a part of the granules was used for granule characterization. The rest of the batch was used as such to produce tablets.

2.4.   Tableting

Tablets were prepared by single compression (no precompression) using a high speed rotary tablet press (MODUL™ P, GEA Pharma Systems – Courtoy™, Halle, Belgium) equipped with ten punches (Ø = 9 mm, flat faced bevel edge, no embossing). In order not to impair Raman and NIR measurements, it was important that all tablets had the same thickness (4 mm), diameter (9 mm) and weight (300 mg). Fill depth (FD) was adjusted before each experiment to obtain the desired weight. Paddle speeds (10–20 rpm), tableting speed (20 rpm) and distance between the punches under compression (3.25 mm) were kept constant. Hence, observed differences in physical properties of the tablets are only caused by the differences in granule characteristics and not by the tableting process parameters. Moreover, several tableting parameters (fill depth, compression force and variability of the compression force) could also be defined as a response of the granule characteristics. Although the fill depth is set at the beginning of each experimental run and kept constant, its absolute value is dependent on the flow properties of the granules. The compression force and its variability are parameters dependent on the compressibility and packing properties of the granules. Mean weight was kept constant for all experiments, but small variations are inherent to the dynamics of the process. Consequently, as weight variability could only be influenced by the granule characteristics (flow properties) since tableting speed and paddle speeds stayed the same throughout all experiments [24], this parameter was also taken into account as a response. The forced feeder was filled with 400 g of granules. The machine was run for 60 seconds and then tablets were sampled during 60 seconds. Room temperature (21 ± 2 °C) and relative humidity (30 ± 2%) were controlled. Tablets were collected in bags, placed in an environmental controlled room (T = 21 ± 2 °C; RH = 30 ± 2%) and allowed to relax for 24 h. Before analysis, 72 tablets out of each bag were placed in tablet trays, with a separate slot for each tablet, assigning them an individual identity. This was preserved through all further analysis (Raman spectroscopy, NIR spectroscopy and reference analysis) to correlate results between different analytical techniques.

2.5.   Design of experiments

The experimental ranges for the Design of Experiments (DoE) factors (granulation parameters: API conc, LFR, BT and SC) were chosen based on a former study [22]. The concentration of theophylline was set at three levels (19.5, 29.25 or 39% (w/w to the dry powder mix)) and achieved by preblending the API, 2.5% PVP and the remaining amount of lactose by low shear mixing. Also the liquid feed rate was varied at three levels (36.2, 41.2 and 46.3 g/min) corresponding to a water concentration of 8, 9 and 10% respectively, calculated on wet mass. The full length of the barrel was preheated, either to 25 or 35 °C. As fourth process parameter, the amount of kneading elements was varied between 4 and 12. When 12 kneading elements were used, two kneading zones each consisting of 6 kneading elements were assembled, separated by a conveying element and an extra conveying element after the second kneading block [25]. For both screw configurations (1×4, 2×6), the angle of the kneading elements was kept constant at 60°.

As the amount of process parameters was relatively low (four) as well as the levels at which they were explored (two or three), a full factorial design was justified. Furthermore, since each level of each process parameter could be combined with each level of another process parameter, the experimental region could be identified as regular, which is a requisite for a (full) factorial design. Since a full-factorial design gives the maximum amount of information compared to other designs as this arrangement enables the effect of one factor to be assessed independently of all the other factors [26], this approach was followed. The combination of 2 factors at three levels and 2 factors at two levels resulted in ($3^2 \times 2^2$) 36 experiments. One repetition of the center point was added, which leads to a total of 37 experiments. An overview of the DoE is given in Table 1.

2.6.   Granule characterization

Particle size analysis was done by sieve analysis, using a sieve shaker (Retsch VE 1000, Haan, Germany). 65 g of granules was placed on the upper sieve of the set (150, 300, 500, 710, 1000, 1400 and 2000 µm) and shaken at an amplitude of 2 mm for 5 min, after which the amount retained on each sieve was determined. Fines and oversized agglomerates were defined as the fractions <300 and >2000 µm, respectively.

Granule friability was determined using a friabilator (Pharma Test PTF E, Hainburg, Germany) at a speed of 25 rpm for 10 min, by placing 10 g ($W_{initial}$) of granules together with 200 glass beads (mean diameter 4 mm) into the drum and subjecting them to falling shocks. Before determination, the granule fraction <150 µm was removed to assure the same starting conditions. After ending a test, the glass beads were removed and the weight of the granules retained on the 150 µm sieve (W_{final}) was determined. Each sample was measured in triplicate. The friability was calculated using Equation (1).

$$\text{Friability (\%)} = \left(\frac{W_{initial} - W_{final}}{W_{initial}}\right) \times 100 \qquad (1)$$

Bulk and tapped density of the granules (30 g) were determined in a 100 ml graduated cylinder. The granules were poured from a height of 40 cm through a stainless steel funnel with a 10 mm orifice into the graduated cylinder, mounted on a tapping machine (J. Engelsmann, Ludwigshafen am Rhein, Germany). The granules were allowed to settle loosely under the influence of gravity and the initial volume (V_0) was recorded. The sample was tapped for 1250 times and the final volume (V_{1250}) was determined. Each sample was measured in duplicate. Bulk (ρ_{bulk}) and tapped (ρ_{tapped}) densities were calculated as 30 g/V_0 and 30 g/V_{1250}, respectively. These values were used to calculate the compressibility index (CI) (Equation (2)) [27].

$$\text{CI (\%)} = \left(\frac{\rho_{tapped} - \rho_{bulk}}{\rho_{tapped}}\right) \times 100 \qquad (2)$$

2.7. Tablet evaluation by reference analyzing techniques

Hardness, thickness and diameter of tablets ($n = 20$) were determined with a semi-automated hardness tester (Sotax HT 10, Basel, Switzerland). The tablet tensile strength (TS) was calculated according to Fell and Newton (Equation (3)) [28].

$$\text{TS (MPa)} = \frac{2 \times F}{\pi \times d \times t} \qquad (3)$$

where F, d and t stand for the diametral crushing force (N), the tablet diameter (mm) and the tablet thickness (mm), respectively.

Tablet friability was determined using a friabilator described in European Pharmacopeia (Pharma Test PTF E, Hainburg, Germany), at a speed of 25 rpm for 4 min. Tablets ($n = 22$) were dedusted and weighed before ($W_{initial}$) and after ending (W_{final}) a test. The percentage weight loss expresses the tablet friability and was calculated using Equation (1). In those cases where cracked, cleaved or broken tablets were detected after friability testing, it was reported in the results that these batches failed the test.

To calculate the porosity (ε) of the tablets, the apparent density (ρ_{app}) of the tablets was determined. Five dimensions of 10 tablets with known weight were measured with a projection microscope (Reickert, 96/0226, Vienna, Austria). Subsequently, the volume of the tablet was calculated according to Equation (4).

$$V\,(mm^3) = \left[\left(\pi \times \left(\frac{D_1}{2}\right)^2 \times H_1\right) \right. $$
$$\left. + 2\left(\frac{1}{3} \times \pi \times H_2 \times \left(\left(\frac{D_2}{2}\right)^2 + \left(\frac{D_3}{2}\right)^2 + \frac{D_2}{2} \times \frac{D_3}{2}\right)\right)\right] \qquad (4)$$

where H_1 and D_1 are the height and diameter of the central cylinder respectively, and H_2, D_2 and D_3 are the height, diameter of lower base and diameter of upper base of the conical frustum (horizontally sliced cone) respectively. Weight divided by the volume of the tablet resulted in the apparent density

(ρ_{app}). Based on the true density of the granules (ρ_{true}) determined by helium pycnometry (Accupyc 1330 pycnometer, Micrometrics Instruments, Norcross, GA, USA), with ten purges and ten runs per measurement ($n = 3$), the porosity of the tablets was calculated according to Equation (5).

$$\varepsilon\,(\%) = \left(1 - \frac{\rho_{app}}{\rho_{true}}\right) \times 100 \qquad (5)$$

Disintegration time (sec) was determined ($n = 6$) using the apparatus described in European Pharmacopeia (PTZ-E Pharma Test, Hainburg, Germany). Tests were performed in distilled water at 37 ± 0.5 °C using disks.

2.8. Prediction of tablet properties using spectroscopic techniques

All 72 tablets from each DoE batch were measured with a NIR-Flex N500 transmission FT-NIR spectrometer (BUCHI, Switzerland) using the NIRWare software. This system contains a tablet holder, isolated from external light sources that can contain up to 10 tablets at a time. The tablet holder minimizes light scattering effects unrelated to the tablet physical properties, providing a robust measurement method. Spectra were collected with 128 scans over the range 11,520 cm^{-1} to 6000 cm^{-1} with a resolution of 4 cm^{-1} and an acquisition time of 38 seconds.

The same tablets were also measured with a RamanRxn2 Analyzer (Kaiser Optical Systems) based on a 785 nm excitation laser with a power of 400 mW and a charged coupled device (CCD). Samples were irradiated from above through a PhAT probe (backscattering geometry) and from underneath (using the transmission accessory), collecting the signal for Raman shifts in the range 150 cm^{-1} to 1890 cm^{-1} with a resolution of 0.3 cm^{-1} and an acquisition time of 15 sec for the backscattering geometry and 55 sec for the transmission geometry. Tablets were placed in an automated tablet holder to minimize light scattering effects unrelated to the tablet physical properties. The probe was fixed at a 25 cm distance from the holder. To prevent background noise, measurements were performed in complete darkness by covering both tablet holder and PhAT probe with a black cover. No human interference was necessary during the measurements, resulting in a very robust procedure.

PCA models were built to provide an overview of the collected data. Individual PLS models were developed for the prediction of the tablets' physical properties (friability, tensile strength, porosity and disintegration time) and also for the prediction of the concentration of theophylline. Models for the physical properties of tablets were developed individually for each concentration of theophylline to minimize the spectral variation originating from the change in the tablets chemical composition. Modeling was performed using SIMCA 13.0.3 (Umetrics, Umeå, Sweden). Given that the physical features of tablets have been described to influence spectra not only on the form of light scattering effects (i.e. baseline offset) but also on peak height or peak shifts, several different pretreatments were tested including Standard Normal Variate (SNV) and Multiplicative Scatter Correction (MSC) [18,20]. First and second derivatives were also applied calculating 15-point

quadratic Savitzky–Golay filters. Several wavenumbers were tested to find the optimal spectral range. The parameters used to examine the PCA models performance were R^2X and Q^2. The performance assessment of PLS models was based on the R^2X, R^2Y, Q^2 and Root Mean Squared Error of Prediction (RMSEP). The normalized RMSEP (nRMSEP) was also calculated. This non-dimensional statistical parameter facilitates the comparison between the errors of models for the prediction of properties with very dissimilar units. The RMSEP was normalized by the range of the measured property according to Equation (6):

$$nRMSEP\,(\%) = \left(\frac{RMSEP}{Y_{max} - Y_{min}} \right) \tag{6}$$

with Y_{max} and Y_{min} as the maximum and minimum values of the property included in the model in question, respectively.

2.9. Influence of granulation parameters on granule properties, tablet properties and tableting process parameters

To demonstrate the effect of granulation process parameters on granulation properties, tablet properties and dependent tableting parameters (fill depth, compression force and variability in compression force), Multiple Linear Regression (MLR) analysis was performed using MODDE 9.1 (Umetrics, Umeå, Sweden).

3. Results and discussion

3.1. Prediction of tablet properties using spectroscopic techniques

3.1.1. Physical properties
PLS models were built separately for each of the measured properties and theophylline contents. Two thirds of the total number of observations was used for the model development while one third was used for its validation. Table 2 depicts the best possible models found for correlating the tablets' physical properties with the collected spectra. It can be observed that no acceptable models could be obtained since the (n)RMSEP values are too high to be considered satisfactory. Even though the models captured almost all spectral variation, mostly it could not be correlated to any of the assayed tablets physical properties and, therefore, no good predictions could be obtained. As an illustration, plots of the observed versus predicted values for the 4 studied properties (tensile strength, friability, porosity and disintegration time) were constructed for the NIR models for an API concentration of 29.25% (Fig. 1).

Earlier studies have shown a correlation between spectral information (both Raman and NIR) and tablet hardness, porosity and disintegration time. However, in these studies, tablets were prepared with the same formulation but compressed at different compression forces yielding tablets with different thickness, diameter and/or weight. Differently, in the current study tableting was performed in a way that all tablets had these properties (thickness, diameter and weight) kept constant. Given this, the differences in physical properties observed between the tablets could only be related to the properties of

the tableted granules (size distribution, friability, amount of fines, amount of oversized particles) and thus are dependent on the granulation parameters as varied in the performed DoE. These findings suggested that the PAT-tools used were not able to capture these differences in physical properties between tablets. Hence, in manufacturing, where the variations in a stabilized process are also limited, changes in tablet characteristics would stay unnoticed. Moreover, it suggests that in research where tablets were compressed with different compression forces, the correlation seen between spectral data and tablet properties was not only due to (detectable) large differences in the extent of bonding and density, but also to differences in the dimensions (thickness) of the measured tablets.

3.1.2. Theophylline content and hydration level
All of the assayed techniques allowed a clear distinction between the 3 concentrations of theophylline in the tablets and also between the levels of theophylline anhydrate and monohydrate. The best PCA models for the visualization of this feature can be observed in Table 3.

Fig. 2 depicts the scores and loadings of the first 2 principal components (PC) of the PCA model obtained from the backscattering Raman data. On the score scatter plot it is possible to observe three different clusters according to PC1. The loadings of PC1 correspond to the difference between the pure analyte spectra of theophylline and lactose. The positive peak at 555 cm^{-1} reveals that with an increase of PC1 scores there is a simultaneous increase of theophylline anhydrate concentration. Moreover, on the loadings of PC2 a positive peak of theophylline monohydrate can be observed at 1686.9 cm^{-1} and a negative peak of theophylline anhydrate at 555 cm^{-1}. With the increase of PC2 scores, theophylline anhydrate content decreases and theophylline monohydrate increases. The PC1 and PC2 loadings of the transmission Raman model are identical and describe the same information as the backscattering mode.

Regarding the PCA model obtained from NIR spectral data, clustering along PC1 is also present (Fig. 3). Three individual clusters can be observed according to the concentration of theophylline. PC1 loadings contain a negative peak around 8900 cm^{-1}, which is characteristic of theophylline and therefore the scores of this component are negatively correlated with the theophylline concentration. On the other hand, PC2 loadings are positive at 8936 cm^{-1}. This peak represents the theophylline hydration level, with higher scores as the theophylline hydration level increases (Fig. 3). These conclusions agree with the findings of Fonteyne et al. [29].

PLS models were also built for the prediction of the theophylline content in the tablets. Forty eight of the 72 observations (tablets) were used from each batch to calculate the models and the remaining observations were used for validation. From all the tested pretreatments and wavenumber ranges the combinations providing the best model for each spectral technique were selected. Table 3 indicated that the captured variance in the spectra and in the theophylline content is similar for all models. The 3 spectroscopic techniques also present identical performance in predicting the content of theophylline with an error of prediction around 1%. A visualization of this predicting performance is given in Fig. 4, with plots depicting the relationship between the observed versus the

Table 2 – PLS models for the prediction of the tablet properties. The range is defined as the minimum and maximum values of the corresponding property measured in the individual tablets.

Physical property	Theophylline concentration (%/tablet)	Spectroscopic technique	Range	Preprocessing	Wavenumber	# PC	R2X (%)	R2Y (%)	Q2 (%)	RMSEP	nRMSEP (%)
TS	19.50	BRaman	0.2 to 2.2 MPa	–	150–1890	2	99.0	17.0	15.8	0.351 MPa	0.181
		TRaman		–	150–1890	2	99.8	11.4	4.6	0.377 MPa	0.194
		NIR		–	8700–9500	5	99.8	40.0	24.7	0.372 MPa	0.192
	29.25	BRaman	0.5 to 2.8 MPa	–	150–1890	1	91.4	7.1	6.1	0.508 MPa	0.217
		TRaman		–	150–1890	2	98.8	27.7	26.8	0.414 MPa	0.177
		NIR		–	8700–9500	2	99.8	5.9	0.3	0.487 MPa	0.208
	39.00	BRaman	0.6 to 3.0 MPa	–	150–1890	7	99.8	52.9	42.0	0.357 MPa	0.146
		TRaman		–	150–1890	4	99.7	21.8	18.5	0.378 MPa	0.154
		NIR		–	8700–9500	2	99.8	2.7	1.3	0.516 MPa	0.211
Friab	19.50	BRaman	0.2 to 10.9%	SNV	150–1890	13	99.2	96.0	93.7	0.868%	0.081
		TRaman		SNV	150–1890	5	96.7	63.4	62.4	2.247%	0.210
		NIR		–	8700–9500	6	100	49.8	47.7	2.401%	0.224
	29.25	BRaman	0.1 to 2.4%	SNV	150–1890	11	99.4	90.1	68.6	0.269%	0.117
		TRaman		SNV	150–1890	10	99.2	98.0	93.1	0.293%	0.128
		NIR		–	8700–9500	6	100	55.1	52.9	0.508%	0.222
	39.00	BRaman	0.1 to 0.3%	SNV	150–1890	13	99.6	94.8	91.7	0.022%	0.118
		TRaman		SNV	150–1890	6	98.9	78.4	77.8	0.027%	0.145
		NIR		–	8700–9500	5	100	48.4	47.5	0.040%	0.214
ε	19.50	BRaman	19.9 to 33.8%	SNV	150–1890	5	97.5	74.8	66.2	1.891%	0.136
		TRaman		–	150–1890	2	99.9	50.9	45.2	1.392%	0.100
		NIR		–	8700–9500	1	88.4	1.7	0.9	4.072%	0.293
	29.25	BRaman	18.8 to 31.5%	SNV	150–1890	10	99.3	91.9	78.3	1.910%	0.150
		TRaman		–	150–1890	4	99.5	39.7	28.2	2.890%	0.228
		NIR		–	8700–9500	4	100	28.7	19.3	3.152%	0.248
	39.00	BRaman	19.1 to 100%	SNV	150–1890	1	55.9	5.4	5.0	6.047%	0.075
		TRaman		–	150–1890	1	92.0	0.6	0.7	5.459%	0.067
		NIR		–	8700–9500	1	98.5	4.4	3.6	5.750%	0.071
Disint	19.50	BRaman	73 to 611 s	1st der.	150–1890	5	96.5	84.2	74.5	69.795 sec	0.130
		TRaman		1st der.	150–1890	7	99.6	99.5	90.7	57.152 sec	0.106
		NIR		–	7500–11520	2	99.2	53.3	42.2	99.805 sec	0.186
	29.25	BRaman	228 to 717 s	1st der.	150–1890	2	83.2	23.9	17.3	94.671 sec	0.193
		TRaman		1st der.	150–1890	3	92.6	36.8	9.3	86.974 sec	0.177
		NIR		–	7500–11520	2	96.3	20.8	9.2	108.875 sec	0.222
	39.00	BRaman	547 to 1590 s	1st der.	150–1890	6	98.0	93.4	83.9	124.085 sec	0.120
		TRaman		1st der.	150–1890	6	98.7	94.5	84.4	134.317 sec	0.130
		NIR		–	7500–11520	2	98.5	67.9	64.3	152.224 sec	0.148

TS, tensile strength (MPa); Friab, friability (%); ε, porosity (%); Disint, disintegration time (sec); BRaman, backscattering Raman; TRaman, transmission Raman; NIR, transmission near-infrared; SNV, standard normal variate; 1st der, 1st derivative; # PC, number of principal components; R2X (%), spectral variance captured by the model; R2Y (%), variance in the measured property captured by the model; Q2 (%), total variation predicted by the model; RMSEP, root mean square error of prediction; nRMSEP (%), normalized root mean squared error of prediction.
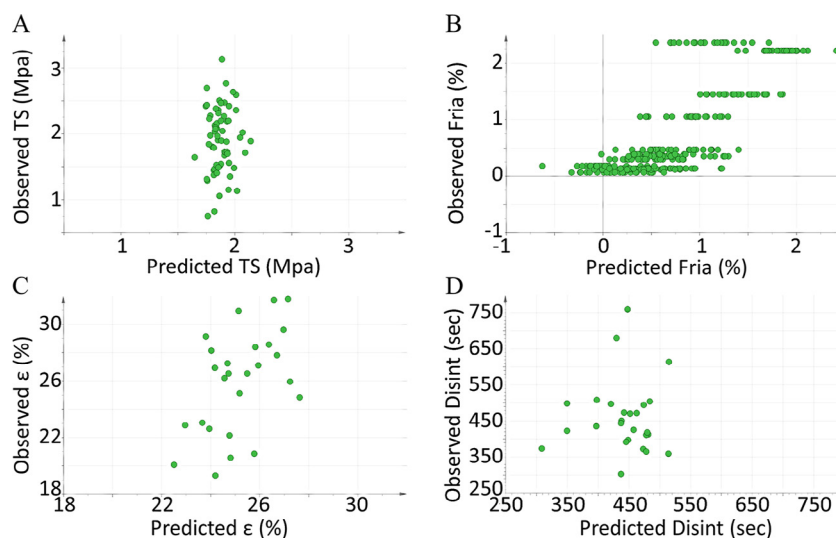
Fig. 1 – Relationship between observed and predicted values for the NIR models for a theophylline concentration of 29.25% of (A) tensile strength (TS), (B) friability (Fria), (C) porosity (ε) and (D) disintegration time (Disint).

predicted theophylline concentrations for all the spectroscopic techniques.

3.2. Influence of granulation process parameters on granule properties

Based on the data of the particle size distribution (PSD), a significant relationship between amount of fines, amount of oversized agglomerates and all four process variables (API %, LFR, BT, SC) was detected (Fig. 5A and B; Table 1). Due to the hydrophobic character of theophylline anhydrate, the formation of liquid bridges was hampered, resulting in smaller particles and hence a larger amount of fines. On the contrary, increasing the liquid feed rate, barrel temperature and the number of kneading elements yielded less fines (4.9–43.3% < 300 µm) and more oversized agglomerates (4.4–43.0% > 2000 µm). Due to a larger amount of available liquid, an increased dissolution rate and a more intensive mixing of powder and granulation liquid, more liquid bridges could be formed between the powders. These results are in accordance with those obtained by other authors [1,22,30–33].

The friability of the granules (4.3–25.9%) was clearly affected by the API %, LFR and SC (Fig. 5C; Table 1). A lower theophylline concentration, higher liquid concentration and more kneading elements resulted in less friable granules. These results could also be linked with the formation of liquid bridges, which are a requisite for strong granules, resisting mechanical stress [22,25,30,32,33].

The granule bulk densities ranged from 0.369 to 0.487 g/ml and the tapped densities from 0.432 to 0.549 g/ml (Table 1). The number of kneading elements was the only process parameter significantly affecting these responses. Increasing the number of kneading elements yielded higher bulk and tapped densities, as more irregular-shaped coarse granules were formed, leading to a better packing [22]. Since the bulk and tapped densities were equally affected by the same process parameter, no significant effect of the process variables on the flow properties, described by the CI, could be detected. Overall,

CIs only differed slightly from each other (7.3–14.6%) (Table 1) and did not exceed 15%, indicating a good flowability of the granules [34]. These conclusions were in agreement with the results obtained by Vercruysse et al. [22] and Djuric and Kleinebudde [33].

3.3. Influence of granulation process parameters on tablet properties and tableting process parameters

The API % was the major factor of influence for all investigated responses. An overview of the results of the tablet analysis is given in Table 1. The responses could be linked not only with the granulation process parameters, but also with the granule characteristics.

For the results of tablet tensile strength, a clear influence of the theophylline concentration and, to a lesser extent, the liquid feed rate could be observed. A higher theophylline concentration and, in accordance with Keleb et al. [35] and Tan et al. [36], a lower water concentration yielded stronger tablets. The hydrophobic character of theophylline anhydrate and a low liquid feed rate during granulation hampered the formation of liquid bridges, resulting in more and smaller particles. As more fines were present, the (extragranular) specific surface area became larger [37–40]. Hence more interaction forces were likely to occur, contributing to higher tablet tensile strengths.

To explain the friability results, the same reasoning as for tensile strength applies. With more fines, the specific surface area increased and allowed more interaction between the granules, hence forming tablets with a higher resistance toward abrasion. This conclusion can be further supported by the observation that 9 out of 12 batches from the lowest API concentration failed the friability test. In these cases cracked, cleaved or broken tablets were detected after friability testing. For the tablets produced with the intermediate API concentration, this was only 4 out of 14. In contrast, none of the batches containing the highest amount of theophylline failed, with friability values ranging from 0.1% to 0.3%.

Table 3 – Selected PCA models for the visualization of theophylline content and hydration level and PLS models for the prediction of theophylline content.

Range (theo conc/tablet)	Model type	Spectroscopic technique	Pre-processing	Wavenumber (cm⁻¹)	#PC	R²X (%)	R²Y (%)	Q² (%)	RMSEP	nRMSEP (%)
17.7% to 41.8%	PCA	BRaman	SNV	400.2–600.9 and 1600.2–1800.9	3	99.4	N/A	99.4	N/A	N/A
		TRaman	SNV	400.2–600.9 and 1600.2–1800.9	3	99.6	N/A	99.6	N/A	N/A
		NIR	MSC	8700–9500	2	99.9	N/A	99.9	N/A	N/A
	PLS	BRaman	–	150–1890	3	99.2	98.4	98.4	0.986%	0.04
		TRaman	SNV	150–1890	3	98.1	98.2	98.2	1.022%	0.04
		NIR	–	8700–9500	3	100	98.0	98.0	1.073%	0.04

BRaman, backscattering Raman; TRaman, transmission Raman; NIR, transmission near-infrared; SNV, standard normal variate; MSC, multiplicative scatter correction; # PC, number of principal components; R2X (%), spectral variance captured by the model; R2Y (%), variance in the measured property captured by the model; Q2 (%), total variation predicted by the model; RMSEP, root mean square error of prediction; nRMSEP (%), normalized root mean square error of prediction.
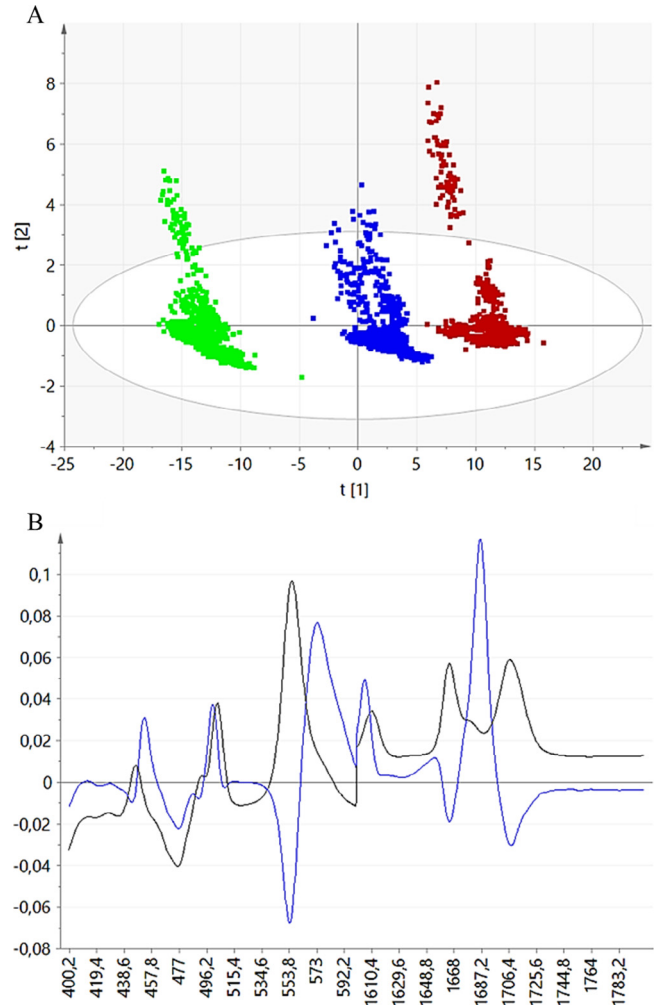

Fig. 2 – (A) Score scatter plot of the first ([t1]) and second ([t2]) principal components of the PCA model on backscattering Raman. Data are colored according to the concentration of theophylline: Red, 19.5%; Blue, 29.25%; Green, 39%; and (B) PC1 loadings (black) and PC2 loadings (blue).

A significant positive influence of API %, LFR and SC on disintegration time was detected. The influence of theophylline concentration could be explained by its hydrophobicity, which hinders the percolation of liquid inside the granules. The effect of the water concentration and the amount of kneading elements could be related to the density of the granules. Higher liquid concentration stimulated the formation of liquid bridges in the granules and kneading elements improved the distribution of granulation liquid, resulting in granules with a higher density [22,25,30,32,33]. The denser tablet structure hampered the percolation of liquids inside the granules, resulting in tablets with a longer disintegration time (108–1576 s). Regarding tablet porosity (20.7–31.5%), API %, LFR and BT were identified as significant process variables. A low level of theophylline and a high level of liquid feed rate and barrel temperate resulted in tablets possessing a high porosity. These observations were also correlated with PSD, as the same set of process parameters yielded less fines. With less fines present,
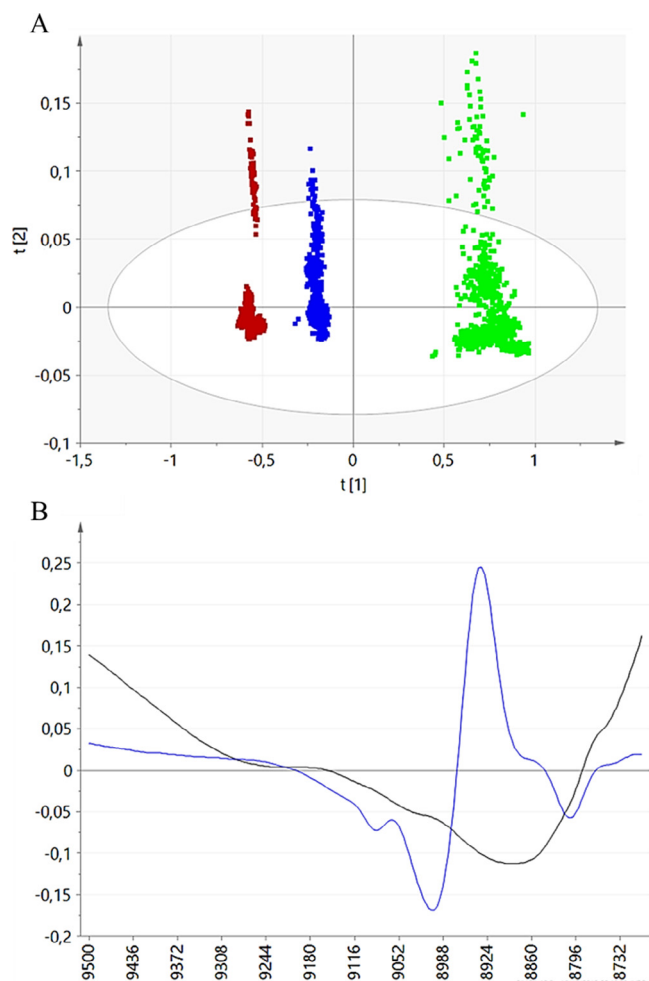
Fig. 3 – (A) Score scatter plot of the first ([t1]) and second ([t2]) principal components of the PCA model on transmission NIR. Data are colored according to the concentration of theophylline: Red, 19.5%; Blue, 29.25%; Green, 39%; and (B) PC1 loadings (black) and PC2 loadings (blue).

filling is a volumetric (and not gravimetric) process, the intergranular space plays an important role. When the theophylline concentration is high, more and smaller particles are present, which are likely to fill this space, hence increasing the variability. However, although significant, the VC for all batches is rather small (<2.5%) and far beneath the typically tolerated 4% limit applied for high speed tableting. These results are all in strong accordance with previously published work on continuous granulation [22], which acknowledges the robustness of this process.

The data of the tableting process parameters (Table 1) identified a correlation between the dependent process parameters (fill depth (FD) (mm), main compression force (MCF) (kN), variation coefficient of main compression force (VC MCF) (%)) and the granule process parameters and resulting granule properties. A significant negative effect of the amount of kneading elements (SC) on fill depth can be detected. More kneading elements had a significant positive effect on bulk and tapped density: at a higher density of the packed granules, a smaller volume (i.e. a lower fill depth) is required to obtain the same weight (300 mg). None of the process parameters had a significant influence on MCF, which is in accordance with the results of CI. Furthermore, since differences in MCF between batches were limited (4.98–6.63 kN), these results illustrate again that all tablets were compressed at the same compression force. It should be mentioned that the absolute value of MCF is rather low, compared to commonly used compression forces (8–16 kN). By keeping this value low, it was possible to obtain tablets with different characteristics brought about by the different granule process parameter settings. At high compression forces, this information is likely lost. A significant positive effect of the API % on VC MCF was observed. These observations were also linked to PSD and tablet weight variability. Although correlated, the VC in tablet weight is much smaller than the VC in MCF, due to the exponential relation between these two tableting parameters.

the intergranular pores during tableting are less likely to be filled, resulting in a lower overall porosity of the produced tablets. For the variation in tablet weight, illustrated by the variation coefficient (VC), the same argumentation can be followed with the API % as the significant process variable. Since die

4. Conclusions

The main goal of this study, which is to predict tablet physical properties from backscattering Raman, transmission Raman and transmission NIR spectroscopic data, was not possible to achieve. The PAT-tools used were not able to capture the differences in physical properties between tablets. This suggests
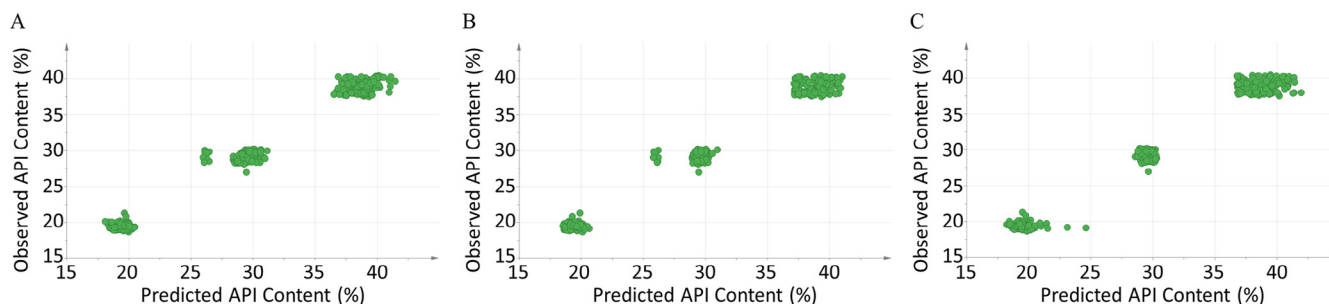

Fig. 4 – Relationship between the observed and predicted theophylline concentration (API content) for (A) backscattering Raman, (B) transmission Raman and (C) NIR.
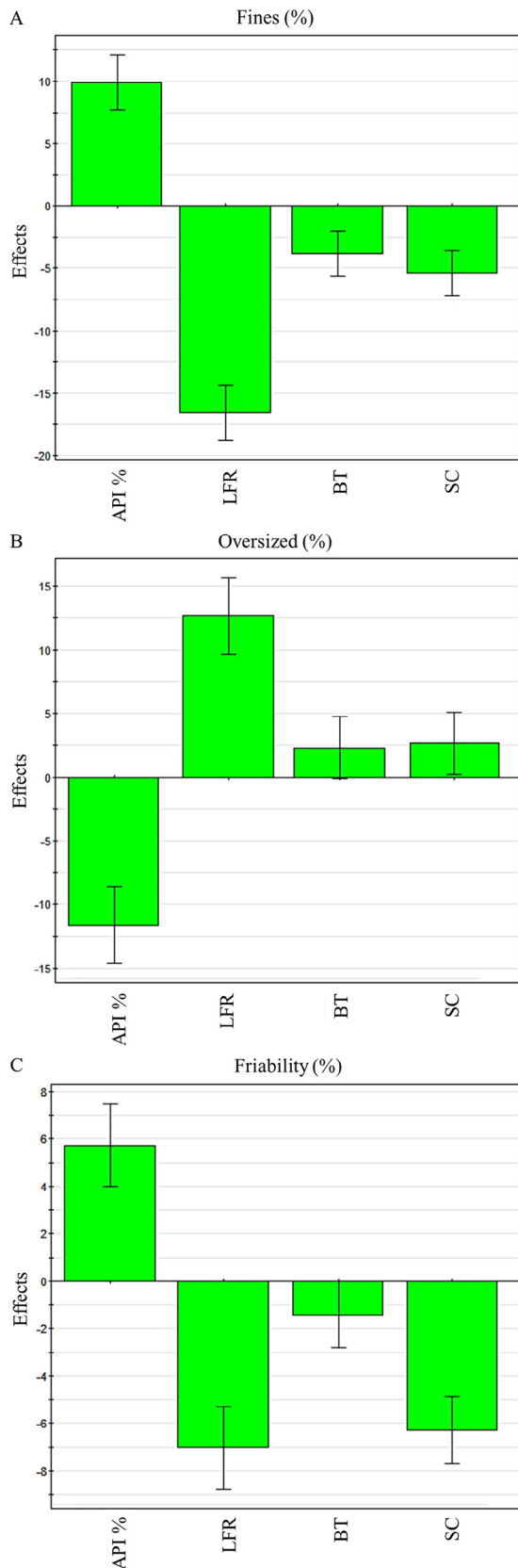
Fig. 5 – Effect plots for particle size distribution of granules ((A) fines, (B) oversized agglomerates) and (C) friability. API %, concentration of theophylline (%); LFR, liquid feed rate (g/min); BT, barrel temperature (°C); SC, number of kneading elements.

that in previous research in which tablets were compressed with different compression forces, the correlation between spectral data and tablet properties was not only linked to differences in bonding and density, but also to differences in tablet dimension (thickness).

In accordance with previous research it was possible to predict the theophylline content by means of a PLS approach. All spectroscopic methods revealed a similar prediction performance with an RMSEP around 1%. PCA models allowed a distinction between the three different levels of theophylline and a determination of the API's hydration level. Furthermore, the effect of several granulation process variables on granule quality, tablet quality and measured tableting parameters was evaluated by means of a DoE. For the granule properties, theophylline concentration and moisture content were identified as the most important parameters. The same effect of theophylline concentration was observed for the tablet properties. The dependent tableting parameters were mainly influenced by the API concentration (VC MCF) and the screw configuration (FD).

Even though it was not possible to predict tablet physical properties with the applied spectroscopic techniques, these PAT-tools have a significant added value when applied for the monitoring of a continuous process since API concentration is an important parameter influencing both granule and tablet properties and it is an important quality attribute for the end product. Based on the good models for this process parameter, implementation of NIR and/or Raman probes in a tablet production line will contribute to the monitoring, adaption and understanding of the process as well as to quality assurance of the end product.

REFERENCES

[1] Fonteyne M, Vercruysse J, Córdoba Díaz D, et al. Real-time assessment of critical quality attributes of a continuous granulation process. Pharm Dev Technol 2011;18:85–97.

[2] Jarvinen K, Hoehe W, Jarvinen M, et al. In-line monitoring of the drug content of powder mixtures and tablets by near-infrared spectroscopy during the continuous direct compression tableting process. Eur J Pharm Sci 2013;48:680–688.

[3] Leuenberger H. New trends in the production of pharmaceutical granules: batch versus continuous processing. Eur J Pharm Biopharm 2001;52:289–296.

[4] Vercruysse J, Delaet U, Van Assche I, et al. Stability and repeatability of a continuous twin screw granulation and drying system. Eur J Pharm Biopharm 2013;85:1031–1038.

[5] Vervaet C, Remon JP. Continuous granulation in the pharmaceutical industry. Chem Eng Sci 2005;60:3949–3957.

[6] Vervaet C, Remon JP. Continuous granulation. In: Parikh DM, editor. Handbook of pharmaceutical granulation technology. New York: Informa Healthcare USA Inc; 2009. p. 308–322.

[7] International Council for Harmonisation of technical requirements for pharmaceuticals for human use (ICH). Topic Q8(R2): Pharmaceutical Development. Geneva, <http://www.ich.org/products/guidelines/quality/article/quality-guidelines.html>; 2009 [accessed 29.12.15].

[8] International Council for Harmonisation of technical requirements for pharmaceuticals for human use (ICH). Topic Q9: Quality Risk Management. Geneva, <http://www

.ich.org/products/guidelines/quality/article/quality
-guidelines.html>; 2005 [accessed 29.12.15].

[9] International Council for Harmonisation of technical
requirements for pharmaceuticals for human use (ICH).
Topic Q10: Pharmaceutical Quality System. Geneva,
<http://www.ich.org/products/guidelines/quality/article/
quality-guidelines.html>; 2008 [accessed 29.12.15].

[10] United States Food and Drug Administration (FDA).
Guidance for industry. PAT – A framework for innovative
pharmaceutical development, manufacturing, and quality
assurance. <http://www.fda.gov/downloads/Drugs/
Guidances/ucm070305.pdf>; 2004 [accessed 29.12.15].

[11] United States Food and Drug Administration (FDA).
Guidance for industry. Process validation: general principles
and practices. <http://www.fda.gov/downloads/drugs/
guidancecomplianceregulatoryinformation/guidances/
ucm070336.pdf>; 2011 [accessed 29.12.15].

[12] Johansson J, Pettersson S, Folestad S. Characterization of
different laser irradiation methods for quantitative Raman
tablet assessment. J Pharm Biomed Anal 2005;39:510–516.

[13] Kessler W, Oelkrug D, Kessler R. Using scattering and
absorption spectra as MCR-hard model constraints for
diffuse reflectance measurements of tablets. Anal Chim Acta
2009;642:127–134.

[14] Chen Y, Thosar SS, Forbess RA, et al. Prediction of drug
content and hardness of intact tablets using artificial neural
network and near-infrared spectroscopy. Drug Dev Ind
Pharm 2001;27:623–631.

[15] Donoso M, Kildsig DO, Ghaly ES. Prediction of tablet
hardness and porosity using near-infrared diffuse
reflectance spectroscopy as a nondestructive method.
Pharm Dev Technol 2003;8:357–366.

[16] Ebube NK, Thosar SS, Roberts RA, et al. Application of near-
infrared spectroscopy for nondestructive analysis of
Avicel® powders and tablets. Pharm Dev Technol 1999;4:19–
26.

[17] Kirsch JD, Drennen JK. Nondestructive tablet hardness
testing by near-infrared spectroscopy: a new and robust
spectral best-fit algorithm. J Pharm Biomed Anal
1999;19:351–362.

[18] Morisseau K, Rhodes C. Near-infrared spectroscopy as a
nondestructive alternative to conventional tablet hardness
testing. Pharm Res 1997;14:108–111.

[19] Shah RB, Tawakkul MA, Khan MA. Process analytical
technology: chemometric analysis of Raman and near-
infrared spectroscopic data for predicting physical
properties of extended release matrix tablets. J Pharm Sci
2007;96:1356–1365.

[20] Donoso M, Ghaly ES. Prediction of tablets disintegration
times using near-infrared diffuse reflectance spectroscopy
as a nondestructive method. Pharm Dev Technol
2005;10:211–217.

[21] Wang H, Mann CK, Vickers TJ. Effect of powder properties on
the intensity of Raman scattering by crystalline solids. Appl
Spectrosc 2002;56:1538–1544.

[22] Vercruysse J, Córdoba Díaz D, Peeters E, et al. Continuous
twin screw granulation: influence of process variables on
granule and tablet quality. Eur J Pharm Biopharm
2012;82:205–211.

[23] Chablani L, Taylor M, Mehrotra A, et al. Inline real-time near-
infrared granule moisture measurements of a continuous
granulation–drying–milling process. AAPS PharmSciTech
2011;12:1050–1055.

[24] Peeters E, De Beer T, Vervaet C, et al. Reduction of tablet
weight variability by optimizing paddle speed in the forced
feeder of a high-speed rotary tablet press. Drug Dev Ind
Pharm 2015;41:530–539.

[25] Van Melkebeke B, Vervaet C, Remon JP. Validation of a
continuous granulation process using a twin-screw
extruder. Int J Pharm 2008;356:224–230.

[26] Eriksson L, Johansson E, Kettaneh-Wold N, et al. Design of
experiments – principles and applications. 3rd ed. Umea:
MKS Umetrics AB; 2008.

[27] Carr RL. Evaluating flow properties of solids. Chem Eng
1965;163–168.

[28] Fell JT, Newton JM. Determination of tablet strength by the
diametral-compression test. J Pharm Sci 1970;59:688–691.

[29] Fonteyne M, Soares S, Vercruysse J, et al. Prediction of
quality attributes of continuously produced granules using
complementary PAT tools. Eur J Pharm Biopharm
2012;82:429–436.

[30] Dhenge RM, Fyles RS, Cartwright JJ, et al. Twin screw wet
granulation: granule properties. Chem Eng J 2010;164:322–
329.

[31] El Hagrasy AS, Hennenkamp JR, Burke MD, et al. Twin screw
wet granulation: influence of formulation parameters on
granule properties and growth behavior. Powder Technol
2013;238:108–115.

[32] Keleb EI, Vermeire A, Vervaet C, et al. Twin screw granulation
as a simple and efficient tool for continuous wet
granulation. Int J Pharm 2004;273:183–194.

[33] Djuric D, Kleinebudde P. Impact of screw elements on
continuous granulation with a twin-screw extruder. J Pharm
Sci 2008;97:4934–4942.

[34] Railkar AM, Schwartz JB. Evaluation and comparison of a
moist granulation technique to conventional methods. Drug
Dev Ind Pharm 2000;26:885–889.

[35] Keleb EI, Vermeire A, Vervaet C, et al. Cold extrusion as a
continuous single-step granulation and tabletting process.
Eur J Pharm Biopharm 2001;52:359–368.

[36] Tan L, Carella AJ, Ren Y, et al. Process optimization for
continuous extrusion wet granulation. Pharm Dev Technol
2011;16:302–315.

[37] Dumarey M, Wikstrom H, Fransson M, et al. Combining
experimental design and orthogonal projections to latent
structures to study the influence of microcrystalline
cellulose properties on roll compaction. Int J Pharm
2011;416:110–119.

[38] Herting MG, Kleinebudde P. Studies on the reduction of
tensile strength of tablets after roll compaction/dry
granulation. Eur J Pharm Biopharm 2008;70:372–379.

[39] Šantl M, Ilić I, Vrečer F, et al. A compressibility and
compactibility study of real tableting mixtures: the impact
of wet and dry granulation versus a direct tableting mixture.
Int J Pharm 2011;414:131–139.

[40] Sun C, Himmelspach MW. Reduced tabletability of roller
compacted granules as a result of granule size enlargement.
J Pharm Sci 2006;95:200–206.